

Srg3, a Mouse Homolog of Yeast SWI3, Is Essential for Early Embryogenesis and Involved in Brain Development

JOONG K. KIM,¹ SUNG-OH HUH,² HEONSIK CHOI,¹ KEE-SOOK LEE,³ DONGHO SHIN,¹
CHANGJIN LEE,¹ JU-SUK NAM,² HYUN KIM,⁴ HEEKYOUNG CHUNG,¹
HAN W. LEE,⁵ SANG D. PARK,¹ AND RHO H. SEONG^{1*}

School of Biological Sciences and Institute of Molecular Biology and Genetics, Seoul National University, Kwanak-gu, Shinlim-dong, Seoul 151-742,¹ Department of Pharmacology and Institute of Natural Medicine, College of Medicine, Hallym University, Chunchon 200-702,² Hormone Research Center, Chonnam National University, Kwangju 500-757,³ Institute of Human Genetics and Department of Anatomy, College of Medicine, Korea University, Seoul 136-705,⁴ and School of Medicine, Sung Kyun Kwan University, Suwon 440-746,⁵ Republic of Korea

Received 21 June 2001/Returned for modification 3 August 2001/Accepted 15 August 2001

Srg3 (SWI3-related gene product) is a mouse homolog of yeast SWI3, *Drosophila melanogaster* MOIRA (also named MOR/BAP155), and human BAF155 and is known as a core subunit of SWI/SNF complex. This complex is involved in the chromatin remodeling required for the regulation of transcriptional processes associated with development, cellular differentiation, and proliferation. We generated mice with a null mutation in the *Srg3* locus to examine its function in vivo. Homozygous mutants develop in the early implantation stage but undergo rapid degeneration thereafter. An in vitro outgrowth study revealed that mutant blastocysts hatch, adhere, and form a layer of trophoblast giant cells, but the inner cell mass degenerates after prolonged culture. Interestingly, about 20% of heterozygous mutant embryos display defects in brain development with abnormal organization of the brain, a condition known as exencephaly. Histological examination suggests that exencephaly is caused by the failure in neural fold elevation, resulting in severe brain malformation. Our findings demonstrate that *Srg3* is essential for early embryogenesis and plays an important role in the brain development of mice.

Modification of the nucleosome structure is a fundamental regulatory process during development. Biochemical and genetic studies have isolated and characterized numerous chromatin-remodeling complexes involved in transcription regulation by modifying histones or altering chromatin structure (1, 30, 33, 51, 57). These complexes can be classified into two major groups, which differ in their use of covalent modification to alter chromatin structure. The first class contains the histone acetyltransferase and histone deacetylase complexes. These complexes regulate the transcriptional activity of genes by determining the level of acetylation of amino-terminal domains of nucleosomal histones which are associated with them. Increased acetylation is usually associated with activation of gene expression, whereas decreased acetylation is associated with repression of gene expression (26, 56). The second class consists of ATP-dependent chromatin-remodeling complexes, which use the energy of ATP hydrolysis to locally disrupt or alter the association of histones with DNA. These complexes contain either SWI2/SNF2 or ISWI-related ATPase associated with various subunits and play roles in both gene activation and repression (30, 57).

The yeast SWI/SNF (ySWI/SNF) was originally identified in *Saccharomyces cerevisiae*. It consists of 11 subunits with a total molecular mass of 2 MDa including SWI2/SNF2 ATPase. Several components have been identified by screening genes in-

involved in the regulation of mating type switching and sucrose-fermenting ability (25, 40). Subsequently, ySWI/SNF genes were shown to be involved in the transcriptional regulation of a wider subset of yeast genes (23). Mutations in both SWI and SNF genes cause pleiotropic phenotypes such as a slow-growth phenotype, defects in mating type switching and sporulation, and inability to utilize sucrose as a carbon source (38, 60). ySWI/SNF has been shown to be highly conserved in all eukaryotes (7, 10, 39, 53). A highly related yeast complex called RSC consists of at least 15 subunits and appears to have a role different from that of SWI/SNF. RSC mutants do not display SWI/SNF transcriptional defects and some, unlike SWI/SNF mutants, are lethal (8).

Homologs of SWI/SNF proteins were identified in *Drosophila melanogaster* (13, 37). The *Drosophila* SWI/SNF complex contains eight major proteins, including the ATPase subunit Brahma (BRM), which is essential for oogenesis and embryogenesis. BRM also plays a particularly important role in the maintenance of homeotic gene expression as a member of the trithorax group (4, 55). BRM complex subunits BAP45/SNR1, BAP155/MOIRA, and BAP60 are conserved between yeast and mammals. MOIRA is a homolog of yeast SWI3 (12, 37). This gene was isolated in three independent screenings for loci that undergo dosage-dependent interactions with *Polycomb* or ectopically expressed *Antennapedia* (29). Mutations in *MOIRA* produce many of the genetic and phenotypic characteristics of BRM mutants (5, 15, 16, 54).

The mammalian SWI/SNF complexes consist of 9 to 12 subunits, with those from different tissues showing significant heterogeneity. Subunit diversity of mammalian SWI/SNF sug-

* Corresponding author. Mailing address: Institute of Molecular Biology and Genetics, Seoul National University, Kwanak-gu, Shinlim-dong, San 56-1 Bldg. 105, Seoul 151-742, Korea. Phone: 82-2-880-7567. Fax: 82-2-887-9984. E-mail: rhseong@plaza.snu.ac.kr.

gests that different complexes might have tissue-specific roles during development (58, 59). The complexes fall into two broad classes, depending on whether they contain human BRM (hBRM) or BRG1 as the ATPase. They contain a core set of components, including the DNA-dependent ATPase SWI2/SNF2, SNF5, and SWI3 homologs (30). A minimum-catalytic-core complex of three SWI/SNF components, BRG1 or hBRM, INI1, and BAF155/BAF170, can remodel both mononucleosome and nucleosome arrays (41). In addition, BRG1 or hBRM alone can substitute for the core complex, albeit with less efficiency. Recent studies of targeted mutations of BRM, BRG1, and SNF5/INI1 in the mouse have expanded the understanding of *in vivo* functions of the mammalian SWI/SNF complex (6, 17, 31, 43, 44). While disruption of mouse *BRM* (*Brm*) produced only mild proliferative effects, deficiency of mouse BRG1 (*Brg1*) or mouse SNF5/INI1 (*Snf5/Ini1*) resulted in peri-implantation death and predisposition of heterozygotes to exencephaly (*Brg1*^{+/-}) and tumor formation (*Brg1*^{+/-} or *Snf5/Ini1*^{+/-}), particularly in the nervous system.

The gene encoding *Srg3*, a mouse counterpart of yeast SWI3, *Drosophila* MOIRA/SWI3D, and human BAF155, was initially isolated as a gene expressed highly in the thymus but at a low level in the periphery by subtractive hybridization (27). *Srg3* is a core component of the SWI/SNF complex in mice, as supported by previous studies with its homologs (37, 41). Interestingly, the expression of antisense RNA to *Srg3* in a thymoma cell line decreased the apoptosis induced by glucocorticoids (GCs), suggesting that this molecule is involved in the GC-induced apoptosis during T-cell development (27). In the present study, we show that *Srg3* is widely expressed during mouse embryogenesis in a spatiotemporal pattern that generally overlaps with that of *Brg1*. Deficiency in *Srg3* expression resulted in early embryonic lethality soon after decidualization by defects in the inner cell mass (ICM) and the primitive endoderm. Similar to *BRG1* knockout mice, *Srg3* heterozygotes are predisposed to exencephaly, suggesting that the SWI/SNF complex plays an important role in brain development.

MATERIALS AND METHODS

Western blotting. Western blotting was carried out as previously described (27). Briefly, whole-cell extracts were separated on sodium dodecyl sulfate (SDS)–7.5% polyacrylamide gel and transferred to nitrocellulose. The membrane was then blocked with Tris-buffered saline–Tween-20 containing 5% non-fat dried milk for 1 to 2 h and incubated with antiserum against *Srg3* or BRG1, which also has been described previously (27), at room temperature for 2 h. Enhanced chemiluminescence reagents (Amersham Pharmacia) were used for detection.

Targeted disruption of *Srg3* and genotyping. The *Srg3* genomic DNA clone was obtained from a mouse 129/Sv genomic library (Stratagene) using a 5' 0.6-kb *XhoI*–*HindIII* fragment of cDNA as a probe. The targeting vector was constructed by cloning a 5.4-kb *BamHI*–*HindIII* genomic DNA fragment encompassing sequences upstream of exon 4 as the long arm and a 1.4-kb *NheI*–*EcoRV* fragment including portions of intron 4 (intron between exons 4 and 5) and exon 5 as the short arm into a neo expression cassette (PGKneoLox2DTA) (49). This vector contains the diphtheria toxin gene driven by the P_{gk} promoter for negative selection. The construct was linearized by *XhoI* digestion and electroporated into 129/Sv-derived AK7 embryonic stem (ES) cells (49). ES cell colonies were selected with G418, and correctly targeted clones were identified by PCR using primers corresponding to the Neo gene (5'Neo; 5'-TCGCAGCGCATCGCCTTCTA-3') and a genomic sequence outside of the targeting construct (3XB; 5'-ATCGTGTCTATTACCCTGATGC-3'). Seventeen PCR-positive clones were obtained from screening 750 G418-resistant clones. Clones identified as homologous recombinants were confirmed by Southern blot analysis using a 5' external genomic probe (see Fig. 3A and B). Eight out of 17 positive clones were

used for microinjection into the C57BL/6J host blastocysts, and all clones gave rise to chimeric mice. To establish heterozygous lines, chimeric males were mated with C57BL/6 females. Germ line transmission of the mutated allele was verified by Southern blotting and three-primer PCR analysis of tail DNA from agouti coat colored F₁ offspring using common 5' primer P1 (5'-ACAACGAAATCTGTGGAGTAGC-3'), in combination with *Srg3*-specific 3' primer P2 (5'-GGGATGGGTCTCTGAAGATCA-3') and *Neo*-specific 3' primer P3 (5'-CTAAGCGCATGCTCCAGAC-3') (see Fig. 3A and C). Primers P1 and P2 amplify a wild-type 450-bp fragment, whereas P1 and P3 amplify a 250-bp fragment specific for the mutant allele. For PCR-based genotyping, embryonic day 3.5 (E3.5) to E8.5 embryos and small pieces of E9.5 to E18.5 embryos underwent lysis by boiling in 10 μ l of lysis buffer containing 0.035 N NaOH and 0.05% SDS.

Blastocyst culture and confocal microscope analysis. E3.5 blastocysts generated from *Srg3* heterozygous intercrosses were collected by uterine flush and individually cultured in Dulbecco's modified Eagle medium supplemented with 15% fetal bovine serum (FBS) in 5% CO₂ at 37°C. For confocal microscope analysis, freshly isolated blastocysts and blastocysts after 3 and 5 days of culture were stained with goat anti-BAF155 (Santa Cruz Biotechnology; sc-9747) and rabbit anti-BRG1 (previously described [27]) antibodies. Fluorescein isothiocyanate-conjugated anti-goat immunoglobulin (IgG) and tetramethyl rhodamine isocyanate-conjugated anti-rabbit IgG secondary antibodies were purchased from Jackson Laboratory. Embryos were then collected and genotyped by three-primer PCR as described above.

Histological analysis and *in situ* hybridization. For paraffin sections, embryos were isolated and fixed in Bouin's solution (Sigma) for 2 to 24 h at room temperature, dehydrated in an ethanol series, cleared in xylene, and embedded in paraffin. Sections were cut 6 to 7 μ m thick and processed for immunohistochemistry or *BF-1* *in situ* hybridization. *In situ* hybridization was carried out as previously described (19, 63). In brief, deparaffinated and rehydrated sections were hybridized at 72°C in a moisture chamber with a digoxigenin-labeled *BF-1*-specific riboprobe. Following hybridization, a high-stringency wash was carried out in 2 \times SSC (1 \times SSC is 0.15 M NaCl and 0.015 M sodium citrate)–50% formamide at 72°C for 1 h. *BF-1* expression was detected with alkaline phosphatase-coupled antidigoxigenin antibodies (Boehringer Mannheim) followed by a reaction with nitroblue tetrazolium and BCIP (5-bromo-4-chloro-3-indolylphosphate). Frozen sections were used for the detection of *Srg3* and *Brg1* expression in mouse embryogenesis. To avoid possible redundancy with the mouse *BAF170* transcript, which is related to *Srg3/BAF155* but encoded by a different gene (59), 0.5-kb *XbaI/PstI* cDNA (nucleotides 2826 to 3309), showing specificity in a BLASTn search, was used as an *Srg3* antisense probe. The *Brg1* probe was prepared as previously described (42).

BrdU labeling and immunohistochemistry. Bromodeoxyuridine (BrdU) (50 μ g/g of body weight) was injected intraperitoneally into pregnant females at E13.5. The mice were sacrificed 2 h after injection, and, for paraffin sections, dissected embryos were fixed in Bouin's solution and processed as described above. The detection of BrdU incorporation was performed in accordance with the manufacturer's instructions (cell proliferation kit; Boehringer Mannheim). For microtubule-associated protein 2 (MAP2) staining, a mouse anti-MAP2 antibody (clone HM-2; Sigma) was used, and the detection was carried out using the LSAB kit (DAKO).

RESULTS

Expression of *Srg3* during mouse development. To examine the expression pattern of *Srg3* during mouse development, Western blotting and *in situ* hybridization experiments were performed. In the embryonic stages, *Brg1* is known to be dominantly expressed about 20- to 30-fold more than *Brm* (43). Thus, we also examined the expression of *Brg1* to address where the SWI/SNF complex is expressed during development. Embryos from E7.5 to E10.5 developmental stages were dissected at the proper times, and whole embryonic extracts were prepared and subjected to Western blotting. Thymocyte extract was used as a quantitative control simply because the *Srg3* protein is most highly expressed in the thymus in adult mice (27). As shown in Fig. 1, *Srg3* is expressed constitutively at a high level in embryonic stages from E7.5 to E10.5, similar to *Brg1* (43). To determine the spatiotemporal pattern of *Srg3* expression and to compare the relative localization of expres-

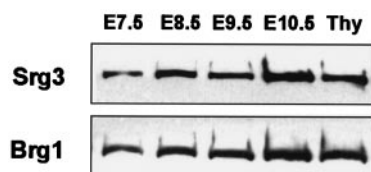


FIG. 1. Expression of *Srg3* and *Brg1* proteins during mouse early embryogenesis. Embryos were dissected at the indicated times (E7.5 to E10.5). To estimate the amount of *Srg3* and *Brg1*, thymocyte extract (Thy) was used as a control. Thirty micrograms of total extract was subjected to SDS-polyacrylamide gel electrophoresis and analyzed by Western blotting. Antisera against *Srg3* and *BRG1* were used as described in Materials and Methods.

sion with *Brg1* expression in mid- and late-embryonic stages from E12.5 to E18.5, in situ hybridization was performed. Frozen sagittal sections of E12.5, E14.5, E16.5, and E18.5 mouse embryos were probed with *Srg3* or *Brg1* cDNA fragments. The expression pattern of *Srg3* overlaps with that of *Brg1*, which is highly expressed in the spinal cord, brain, and thymus as previously reported (42), and *Srg3* appears more ubiquitously than *Brg1* (Fig. 2). At E12.5 and E14.5 (Fig. 2A and C), high expression of *Srg3* is apparent in almost all developing organs except the heart and liver. At E16.5, high expression of *Srg3* is evident in the lung and intestine as well as the central nervous system (CNS) and thymus (Fig. 2E), where *Brg1* is also highly expressed (Fig. 2F). This overall expression pattern of *Srg3* is shown to be altered as the embryos grow to near birth in such a way that the level of expression gradually diminishes. At E18.5, *Srg3* expression appears to be restricted mostly to the CNS and thymus, where *Brg1* is also expressed (Fig. 2G and H, respectively).

Targeted disruption of *Srg3*. To investigate the role of the *Srg3* protein in vivo, we created an *Srg3* null mutation via homologous recombination in mouse ES cells. A targeting vector that replaces a 0.9-kb *HindIII-NheI* fragment including exon 4, which encodes amino acid residues 131 to 158, with the neomycin resistance gene (*Neo*) was used (Fig. 3A). Correct homologous recombination in ES cells was confirmed by Southern blot analysis (Fig. 3B). Since remaining exons 3 and 5 are out of frame, this deletion is expected to result in a null allele. Eight different *Srg3*^{+/-} ES cell clones were independently injected into blastocysts and gave rise to germ line-transmitting chimeric mice that were crossed into a C57BL/6 background. The resulting *Srg3*^{+/-} mice appeared normal and fertile. Genotyping progeny from heterozygous intercrosses was performed by Southern blotting; however, we could not find any homozygous mutants in postnatal progeny. Homozygous embryos were found at the blastocyst stage by three-primer PCR analysis (Fig. 3C). Immunohistochemical analysis of blastocysts confirmed the absence of protein in homozygous mutants (Fig. 4A). The expression of the *Srg3* protein in heterozygous mice was reduced to about one-half the level in control mice in the thymus and developing brain (Fig. 3D), where the *Srg3* protein is highly expressed (27). Thymocytes expressing reduced levels of *Srg3* displayed reduced sensitivity to GC-induced apoptosis (data not shown).

Early embryonic lethality of homozygous mutant. Heterozygous mice were intercrossed in an effort to generate homozy-

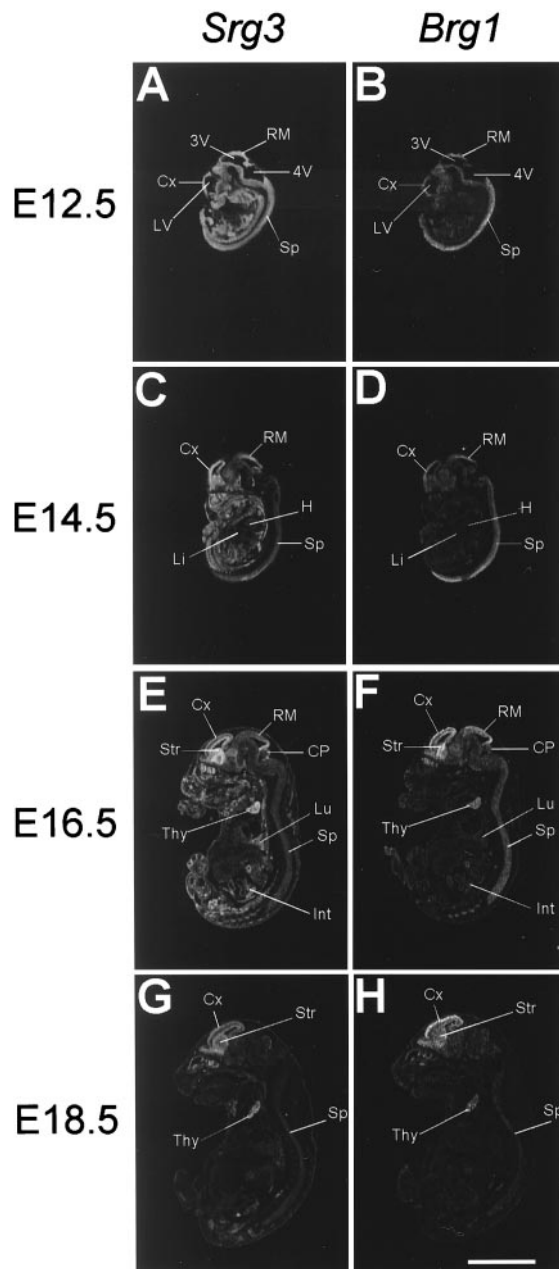


FIG. 2. In situ hybridization analysis of *Srg3* (A, C, E, and G) and *Brg1* (B, D, F, and H) expression at E12.5 (A and B), E14.5 (C and D), E16.5 (E and F), and E18.5 (G and H). Sagittal sections of indicated embryos were hybridized with *Srg3*- or *Brg1*-specific probes. To avoid possible redundant signals with the mouse *BAF170* transcript, the *Srg3* antisense probe was made of the nonredundant region (see Materials and Methods). A sense strand probe was also made, and no signal was detected (data not shown). Cx, cerebral cortex; LV, lateral ventricle; RM, roof of midbrain; 3V, third ventricle; 4V, fourth ventricle; Sp, spinal cord; H, heart; Li, liver; Lu, lung; Int, intestine; CP, cerebellar primordium; Str, striatum; Thy, thymus. Scale bar, 5 mm.

gous mutant progeny. However, no homozygous mutants were identified in the resulting progeny at times ranging from E7.5 to the postnatal stage, and about 26 to 27% (95 of 359) of the decidua from E7.5 to E18.5 were empty or resorbed (Table 1).

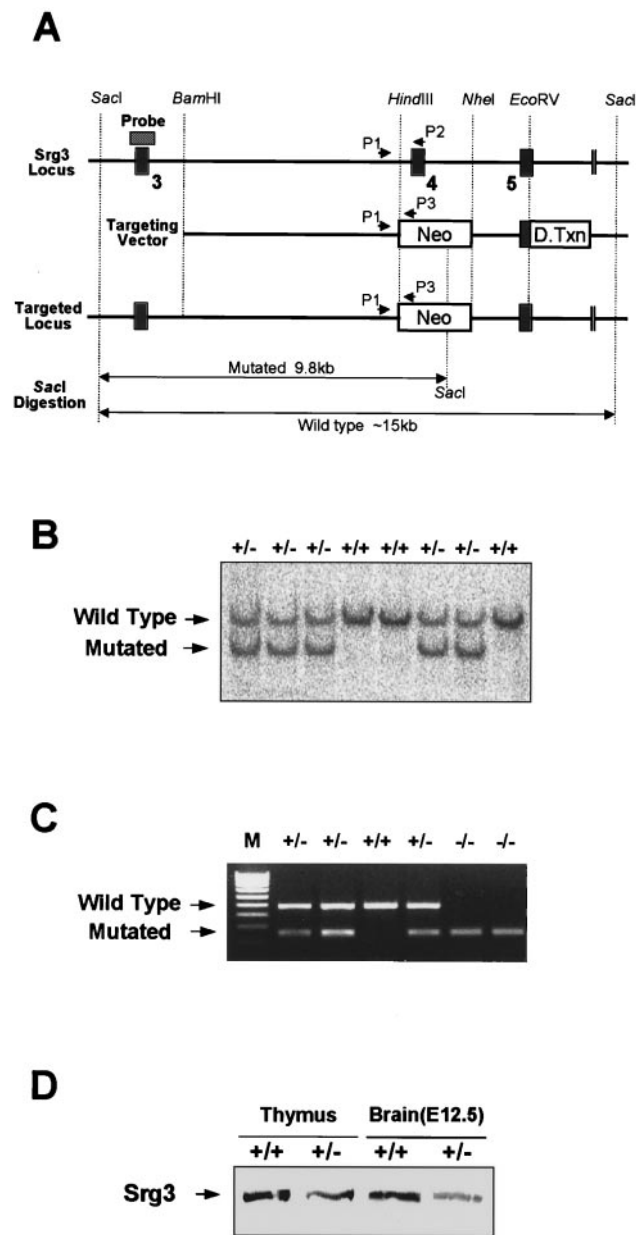


FIG. 3. Targeting of the *Srg3* gene. (A) Schematic diagram of the *Srg3* locus and targeting vector and predicted structure of targeted *Srg3* allele. Restriction enzyme sites and three exons (3 to 5; black boxes) are shown. The locations of the 5' flanking Southern probe (hatched box) and PCR primers (P1 to P3) used in panels B and C are indicated. The targeting construct was designed to replace an exon (exon 4) with a *PGK-Neo* gene. Neo, neomycin resistance gene; D.Txn, diphtheria toxin gene. (B) Southern blot analysis showing correct targeting of the *Srg3* locus. Genomic DNA samples were prepared from tails of the progeny derived from *Srg3* heterozygous intercrosses, digested with *SacI*, and probed as indicated. The resulting 15- and 9.8-kb bands correspond to the wild-type and mutated genotypes, respectively. (C) Three-primer PCR analysis of blastocysts from *Srg3* heterozygous intercrosses showing wild-type (450-bp) and mutated (250-bp) alleles. M, 100-bp marker. (D) Western blot analysis of *Srg3* and *Brg1* expression in the thymus (4 to 6 weeks old) and brain at E12.5 from wild-type littermate and *Srg3* heterozygous mice.

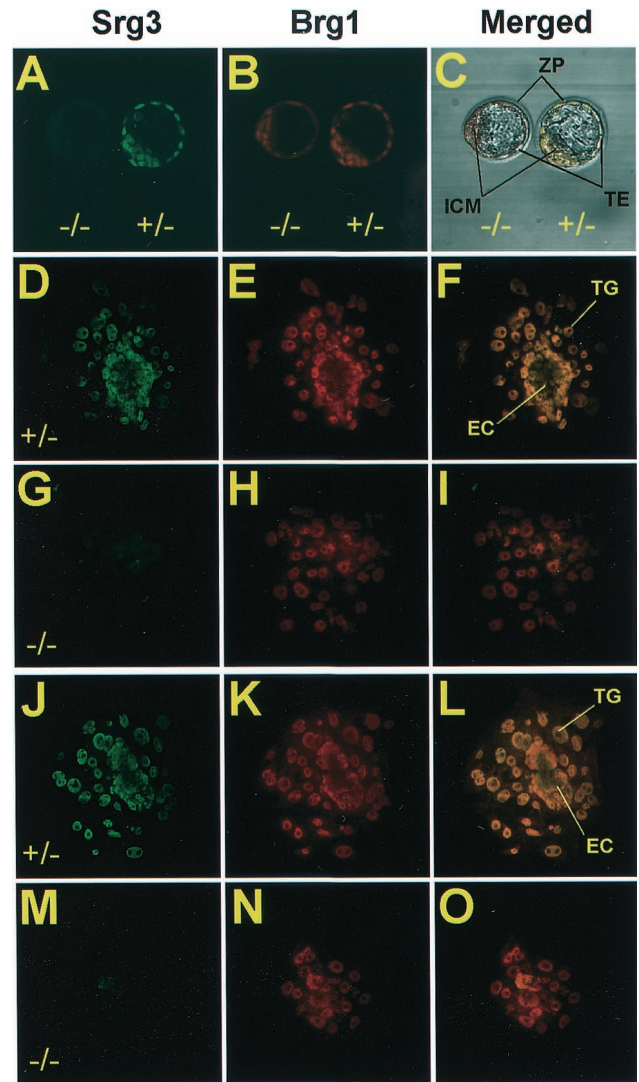


FIG. 4. In vitro outgrowth defects of *Srg3*^{-/-} blastocysts. Freshly isolated blastocysts at E3.5 from *Srg3* heterozygous intercross were directly stained (A to C) or cultured for 3 (D to I) and 5 (J to O) days in Dulbecco's modified Eagle medium supplemented with 15% FBS followed by staining with anti-*Srg3* and anti-BRG1 antibodies. Confocal images of each stage show *Srg3* (A, D, G, J, and M) and *Brg1* (B, E, H, K, and N) expression patterns. Merged images are also provided (C, F, I, L, and O). In the blastocyst stage, *Srg3* null mutants appeared morphologically normal (C); however, after culture for 3 (D to I) and 5 (J to O) days, they failed to form the three-dimensional egg cylinder structure enclosed by the primitive endoderm (I and O). ZP, zona pellucida; TE, trophoctoderm; TG, trophoblast giant cells; EC, egg cylinder.

Histological analysis of E5.5 and E6.5 decidua from heterozygous intercrosses showed that about 28% (11 of 39) of them were empty or seemed to contain traces of degenerated embryos mixed with maternal blood cells (data not shown). These empty decidua are presumed to be *Srg3* homozygous mutant embryos if one assumes a normal Mendelian distribution of genotypes in the F₁ generation. To examine this assumption, the homozygous mutants recovered at the blastocyst stage (E3.5) were cultured in vitro. Very recently, it was reported

TABLE 1. Summary of genotypes resulting from *Srg3*^{+/-} intercrosses

Stage	No. of mice with genotype:				Total
	+/+	+/-	-/-	ND ^a	
Postnatal	131	185	0		316
E9.5–E18.5	61	126 (24 ^b)	0	71 ^c	258
E7.5–E8.5	26	51	0	24 ^d	101
E3.5	22	45	20	3 ^e	90

^a ND, not determined.
^b Number of embryos with neural tube defects resulting in exencephaly.
^c Resorption.
^d Empty decidua.
^e Genotyping failure.

that *Brg1* null mutant dies during the peri-implantation stage, and in vitro blastocyst outgrowth studies revealed that neither the ICM nor the trophoectoderm survives (6). Because *Srg3* is a core component of the SWI/SNF complex, it is presumed that *Srg3* null mutants die from the lack of the activity of the complex. Freshly isolated blastocysts were stained by anti-BAF155, which is also reactive to *Srg3*, and anti-BRG1 antibodies. As shown in Fig. 4A to C, the *Srg3*-deficient blastocyst appears morphologically normal. The *Brg1* protein in the homozygous mutant was stained almost at the same level as that of the heterozygous control, indicating that the lack of *Srg3* does not greatly affect the *Brg1* protein level. To pursue the developmental defect(s) of the *Srg3* homozygous mutant, we cultured blastocysts from heterozygous intercrosses in individual microdrops of medium containing 15% FBS. After 3 to 5 days of culture, wild-type and heterozygous mutant blastocysts hatched from the zona, adhered, and developed into a giant trophoblast layer around the incipient egg cylinder, which consists of the developing ICM and primitive endoderm cells (Fig. 4D to F and J to L). However, the *Srg3*-deficient embryo failed to form the egg cylinder structure and had a few dispersed ICMs and no discernible visceral endoderm layer (Fig. 4G to I and M to O). Stable *Brg1* expression was also detected in cultured embryos (Fig. 4H and N). Compared to the lethality of the *Brg1* null mutant, it is notable that *Srg3*-deficient embryos undergo hatching and partial outgrowth with normal trophoblast giant cell differentiation ex vivo.

Exencephaly in a portion of heterozygous mutants. Interestingly, about 20% (24 of 126; Table 1) of *Srg3* heterozygous embryos exhibit exencephaly. It is well known that almost all exencephaly of genetic origin is caused by neural tube defects (NTDs), causing failure in neural fold elevation followed by outward expansion of neural tissue via the eversion of the neural plate (18). Normally, the neural tube begins to close at E8.5 and completes closure by E9.5 in mice. Gross morphological analysis at E9.5 revealed that some heterozygous embryos display the failure of neural fold elevation (Fig. 5A and B). Subsequently, a severe abnormal brain structure with a failure of neural plate closing in the mid-hind cephalic region is apparent at E10.5 (Fig. 5C and D). Further analyses of the brain structure at E12.5 and E16.5 revealed severe gross perturbations of the whole cephalic structure including extensive malformation of the forebrain (Fig. 5E to H).

To characterize this brain abnormality at the histological level, comparable coronal sections through the forebrains of

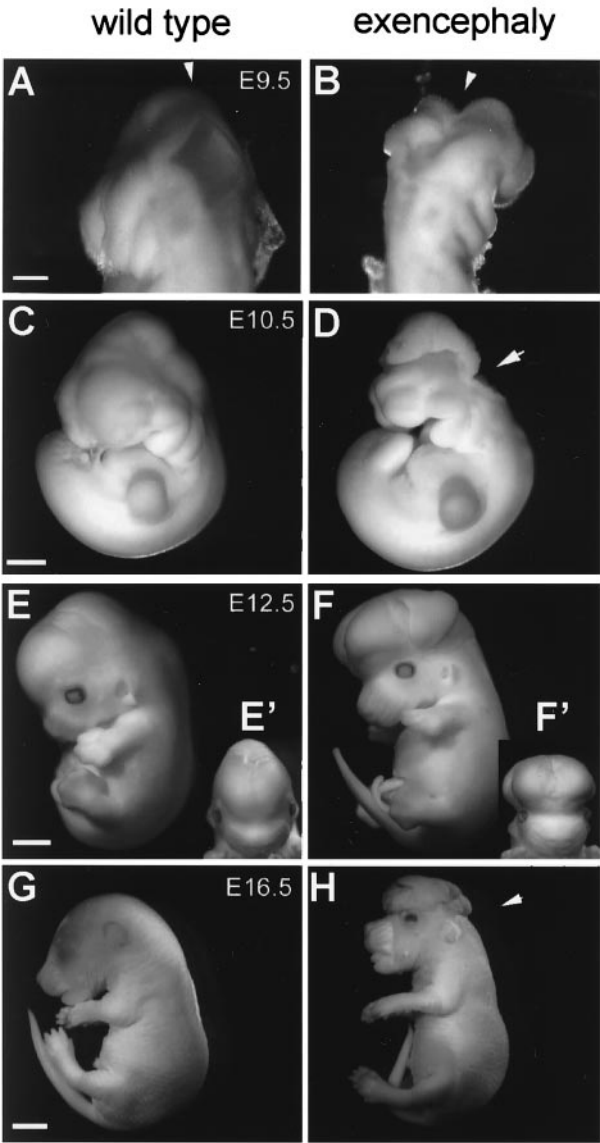


FIG. 5. Gross appearance of wild-type littermates (A, C, E, and G) and exencephalic *Srg3*^{+/-} (B, D, F, and H) mice. (A and B) Dorsal view of E9.5 embryos. In this stage, wild-type embryos show normally closed neural tubes (A, arrowhead). In contrast, the exencephalic embryo shows an open neural tube (B, arrowhead). (C and D) Lateral view of E10.5 embryos. Note the defects in the midbrain-hindbrain junction region (D, arrowhead). (E and F) E12.5, lateral view. (E' and F') Frontal view. Exencephalic embryos show laterally swollen brains (F'). (G and H) E16.5, lateral view. Note the typical exencephaly without the skull (H, arrowhead). Scale bars, 0.2 (A and B); 0.4 (C and D), 1 (E and F), and 2 mm (G and H).

wild-type littermate and exencephalic embryos at E12.5 were stained with hematoxylin and eosin (Fig. 6A and B). In the exencephalic embryo, the third ventricle was clearly open (Fig. 6B) and the diencephalon had burst out to the upper side of the head (Fig. 6A and B), accompanied by the lateral ventricles turned inside out (Fig. 6B). Furthermore, the stenosis of the lateral ventricles in the exencephalic mutant was evident, as well as prominent expansion of the corpus striatum mediale (Fig. 6B and D). To clarify the identity of the telencephalic

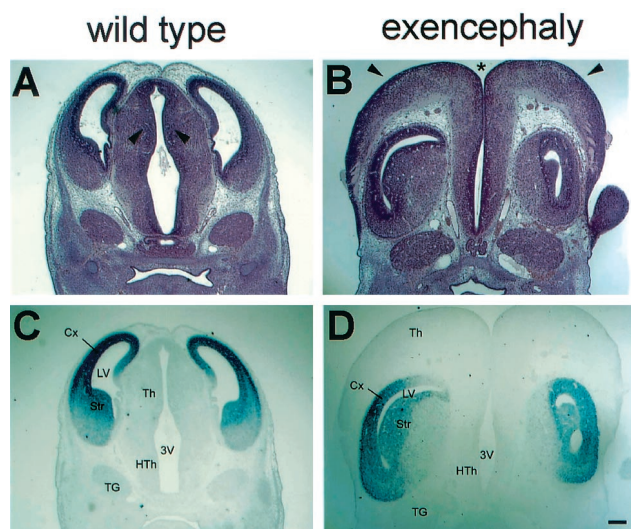


FIG. 6. Histological analysis and *BF-1* in situ hybridization of exencephalic *Srg3*^{+/-} embryos at E12.5. (A and B) Hematoxylin- and eosin-stained coronal brain sections of wild-type littermate and exencephalic embryos. Note the open third ventricle (asterisk), expansion of the thalamic cells (arrowheads) covering the upper side of the head, and shrunken lateral ventricles in the exencephalic embryo (B). (C and D) *BF-1* in situ hybridization of sections adjacent to those shown in panels A and B, respectively. Note that the cerebral cortex is turned upside down. The cerebral cortex appears to be pushed by the enlarged thalamus bursting out to the upper side of the head, with an open third ventricle in the exencephalic embryo. Cx, cerebral cortex; LV, lateral ventricle; Th, thalamus; HTh, hypothalamus; 3V, third ventricle; Str, striatum; TG, trigeminal ganglion. Scale bar, 0.2 mm.

region in exencephaly, *BF-1* (*brain factor-1*), in situ hybridization was performed. *BF-1* is a molecular marker gene whose expression is restricted within the developing basal telencephalon and cerebral cortex (19, 24). In situ hybridization with the *BF-1* gene of exencephalic embryos showed that the telencephalic neuroepithelia were located below the thalamus (Fig. 6D). Additionally, the ganglionic eminence of the exencephalic embryo exhibited a rotation toward the midline axis of the brain, so that the eminence region faces outward from rather than inward to the brain. These observations suggest the possibility that *Srg3* plays an important role during brain development, probably in a dosage-dependent manner. High expression of the *Srg3* protein during E8.5 to E9.5 (Fig. 1), when the neural tube closes, and prolonged constitutively high expression in the CNS region thereafter (Fig. 2) are compatible with this possibility. Recent studies revealed that BRG1 and BAF155 interact with the retinoblastoma suppressor gene product (Rb) and cyclin E, indicating that they participate in the control of the cell cycle (47, 50, 64). Therefore, we investigated the proliferation of the neuroepithelial cells in exencephalic embryos at E13.5 by BrdU labeling. At this stage, developing neuroepithelial cells proliferate within the ventricular zones and subsequently migrate out of this zone to become fully differentiated mature neurons expressing neuronal marker MAP2 (11). Control littermate embryos showed normal neuronal proliferation and differentiation (Fig. 7A, C, E, and F). However, in exencephalic embryos, expression of MAP2 was shown to be relatively reduced in the telencephalic striatum region (Fig. 7B and D). In addition, ectopic proliferating cells were found in the

upper posterior region (Fig. 7B, D, G, and H). These cells appear to be neuronal epithelial cells producing an excessive cell mass in the diencephalic region. It was also found that the mesenchymal tissues of exencephalic embryos were obviously expanded (Fig. 7D). Our observations suggest that the haplo-insufficiency of *Srg3* results in a susceptibility to brain malformation accompanied by inappropriate cellular proliferation and differentiation.

DISCUSSION

Here we report the first study addressing the in vivo role of *Srg3*, a mouse counterpart of yeast SWI3, *Drosophila* MOIRA, and human BAF155. *Srg3* is expressed ubiquitously in postimplantation embryos with particularly high levels of expression in the CNS and thymus. *Srg3* deficiency results in peri-implantation lethality, resulting from a defective development of the ICM and primitive endoderm, as suggested by blastocyst outgrowth studies. Similar to *Brg1*-deficient mice, heterozygotes are predisposed to exencephaly (6). Histological analysis of brains of exencephalic embryos reveals defects in proliferation and differentiation of neural cells, implying that the CNS is sensitive to *Srg3* dosage. Previous studies reported that both *Brg1* and *Snf5/Ini1* heterozygous mice were susceptible to spontaneous neoplasia (6, 17, 31, 44). However, we have not

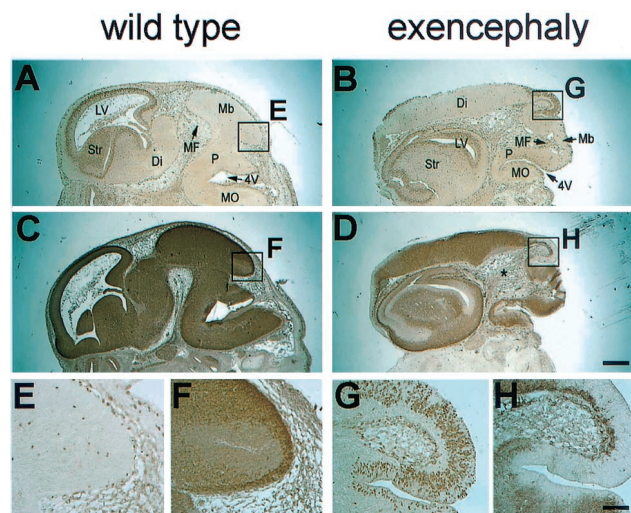


FIG. 7. Neuronal cell proliferation and differentiation of wild-type littermate and exencephalic embryos at E13.5. Sagittal sections are shown. (A and B) BrdU incorporation of the littermate control and exencephalic embryo, respectively, after a 2-h pulse. (C and D) MAP2 staining of sections adjacent to those shown in panels A and B, respectively, showing differentiation of neuronal cells. Note the ectopic proliferating cells in the upper posterior region (box G in panel B). These cells are thought to be the diencephalon-producing neuroblasts. Note also the irregular position of midbrain flexure (MF), open fourth ventricle (4V), and enlarged head mesenchyme (D, asterisk) in the exencephalic embryo (B and D). (E and F) High-power views of the upper posterior regions of panels A and C, respectively, showing the posterior part of midbrain in the control embryo. (G and H) High-power views of the upper posterior regions of panels B and D, respectively, showing the ectopic proliferating cells in the exencephalic embryo. LV, lateral ventricle; Str, striatum; Di, diencephalon; MF, midbrain flexure; Mb, midbrain; P, pons; 4V, fourth ventricle; MO, medulla oblongata. Scale bars, 0.5 (A and D) and 0.1 mm (E and H).

yet looked for such a phenotype although it might be expected in light of the *Brg1* and *Snf5/Ini1* knockout results.

The similar expression patterns of *Srg3* and *Brg1* and the resemblance of the phenotypes of the knockout mice strongly suggest that *Srg3*, as previously shown for *Brg1* and *Snf5/Ini1*, is required for full activity of mammalian SWI/SNF complexes in vivo (6, 17, 31, 44). Further, the present study confirms the essential function of *Srg3*/SWI/SNF in peri-implantation development and control of neural cell differentiation and proliferation.

Comparison of the *Srg3* expression pattern with that of *Brg1* in embryogenesis. The expression pattern of *Srg3* largely overlaps with that of *Brg1* but appeared to be more ubiquitous. From E7.5 to E10.5, both *Srg3* and *Brg1* were expressed at constitutively high levels. During this period, embryos undergo gastrulation, neurulation, and early organogenesis, in which exclusive cell proliferation and differentiation occur. High *Srg3* and *Brg1* expression is consistent with the presumptive need for the SWI/SNF complex to regulate the expression of various genes by remodeling the chromatin structure. In situ hybridization studies using middle- and late-stage embryos (Fig. 2) revealed widespread expression of *Srg3* mRNA in developing embryonic tissues. The expression patterns of *Srg3* and *Brg1* appeared to be similar but somewhat different during mouse embryogenesis. Whereas *Brg1* is highly expressed in some restricted organs such as the brain, spinal cord, and thymus, *Srg3* shows a pattern of high expression additionally in the ventral parts including the lungs and intestines of the developing embryos (Fig. 2). Interestingly, this overall high expression pattern gradually weakened as the embryo neared birth. These observations suggest that there may be an unknown function of *Srg3* independent of *Brg1* in mouse development. Previously, it was reported that Brm is expressed at very low levels at all stages of development in the embryonic tissue (35, 43). On the basis of these findings, it is possible that some *Srg3* proteins may not be components of either *Brg1*- or Brm-containing SWI/SNF complexes in some tissues. It is also worthwhile to note that certain human cell lines containing very little or no BRG1 and hBRM express BAF155 (58). In addition, MOIRA, a *Drosophila* counterpart of *Srg3*, also exhibited an expression pattern which overlaps with those of *BRM* and *SNR1* but which is more widespread (12). These findings support the possibility that *Srg3* may have an alternative novel function(s) besides being a subunit of the SWI/SNF complex.

An essential role for *Srg3* in early embryogenesis. A previous study of yeast demonstrated that a mutation in *SWI3* and *SWI2* resulted in identical phenotypes (38). In *Drosophila*, the SWI3 homolog MOIRA appears to be essential for BRM function in vivo, and mutation of the corresponding genes resulted in identical phenotypes, i.e., homozygous mutants die at the unhatched-larva stage (12, 37). These observations suggest that *Srg3* knockout represents inactivation of the SWI/SNF complex. We demonstrated here that *Srg3* is required for peri-implantation development. In vitro culture of *Srg3*-deficient embryos showed that the trophoectoderm developed into trophoblast giant cells, but no visceral endoderm and egg cylinder formation was found. Recently, it was reported that *Brg1* null mutant died during the peri-implantation stage (6). *Brg1*-deficient embryos did not undergo even hatching processes, and neither the ICM nor the trophoectoderm survived in vitro.

Although *Srg3* and *Brg1* mutants showed similar phenotypes of very early embryonic lethality, there appears to be a time gap in the death of the two mutants. The mutants showed differences in blastocyst hatching and differentiation of the trophoectoderm into trophoblast giant cells. As shown in Fig. 4B, the *Brg1* protein seems to be stable in *Srg3*-deficient embryos. Therefore, it is likely that a basal chromatin-remodeling activity due to BRG1 alone (41) is present in *Srg3* null mutants. This may have caused the phenotypic difference between the *Brg1*-deficient and *Srg3*-deficient mutants. The robust activity of the SWI/SNF complex may be required for the development of the ICM and primitive endoderm into the egg cylinder. However, *Snf5/Ini1* null embryos display defects in the hatching process similar to those displayed by *Brg1* null mutants (6, 17, 31). It is not clear at present what causes the time gap in death between *Srg3* null and *Snf5/Ini1* null embryos. It is possible that *Snf5/Ini1* is more critical for the activity of *Brg1* in vivo at the peri-implantation stage. This possibility needs to be further investigated. In addition, it should be noted that *Brg1*-deficient embryos have Brm-containing SWI/SNF complexes. Although Brm has been shown to be dispensable for mouse development (43), one cannot exclude the effect of the Brm-containing SWI/SNF complex on normal embryogenesis. In fact, there seems to be a correlation between cellular differentiation and expression of BRM (36). Therefore, it is possible that the failure of *Brg1*-deficient blastocysts to develop further may be due to the remaining Brm complex, which does not favor the cellular proliferation required for embryonic development.

Predisposal to exencephaly in the heterozygous mutant. Another conspicuous phenotype of the *Srg3* mutant is exencephaly in a portion of heterozygous embryos. This brain anomaly seems to be due to NTDs, reflecting failure in neural fold elevation. In fact, it is well known that most exencephaly or spina bifida aperta of genetic origin is caused by failure in neural fold elevation (18). However, for most mouse NTDs, it is not clear how the genes involved in NTDs contribute to neural fold elevation (28).

The SWI/SNF complex has been implicated in the regulation of cellular growth and proliferation (36, 57). For example, the BRG1-containing SWI/SNF complex is inactivated by phosphorylation of BAF155 and BRG1 during the G₂/M phase of the cell cycle (48), whereas Brm knockout mice show increased cell proliferation (43). Several studies carried out with human cell lines have shown that BRG1 and hBRM physically interact with Rb. These studies showed that the SWI/SNF complex induced the growth arrest of cells in an Rb-dependent manner (14, 50). In addition, BRG1 and BAF155 have been shown to coimmunoprecipitate with cyclin E. It was revealed that the cdk2-cyclin E complex can phosphorylate both proteins (47). These features of the SWI/SNF complex suggest that the predisposal to NTDs in *Srg3* heterozygous embryos may be due to a failure in cell cycle regulation caused by haploinsufficiency of *Srg3*. Exencephalic embryos showed excessive increases in the number of diencephalic neuronal cells flowing over to the cranial region (Fig. 6). BrdU incorporation and MAP2 staining studies showed that some actively proliferating cells in the upper posterior region seemed to produce an excessive cell mass of the diencephalon and relatively poorly differentiated telencephalic neuronal cells in the striatum (Fig.

7). It is not clear whether these are causes or results of NTDs. However, there seems to be a correlation between abnormal cell proliferation and/or differentiation and NTDs. Studies with some NTD mutants suggest that genes with a basic mitotic function also have a function specific to neural fold elevation (2, 20, 22, 46).

Recently, it was reported that Brg1 is highly expressed during embryogenesis, including the neurulation stage, and that high-level accumulation of its transcript is observed in the spinal cord and brain after neural tube closure (42, 43). Furthermore, *Brg1* heterozygotes also show susceptibility to exencephaly with almost the same penetrance (15 to 30% of heterozygous mutants) (6) as that of *Srg3* heterozygotes. Thus, it is likely that reduced *Srg3* protein expression might result in down-regulation of Brg1-containing SWI/SNF complexes, causing cell cycle perturbation and resulting in NTDs.

Another possible cause of NTDs in *Srg3* heterozygous mutants could be based on the fact that the SWI/SNF complex contains actin itself and an actin-related protein such as BAF53 (59). Some genes in a growing list of mouse NTD mutants have been shown to play roles in the organization of actin molecules in the cytoskeleton (3, 9, 21, 32, 34, 52, 61, 62). It was suggested that part of the force required to change the shape of the neural folds from flat or convex to concave or elevated is a "pulse-string" rearrangement of actin at the luminal-apical surface, changing the neuroepithelial cells from columnar to wedge shaped (45). Thus, it is possible that the SWI/SNF complex may participate in neural fold elevation by its actin-related property or by regulation of some genes organizing actin rearrangement. Whether it is cell cycle regulation, an actin-related property, or another unknown mechanism, the fact that the haploinsufficiency of *Srg3*, as well as of Brg1, confers susceptibility to NTDs indicates the quantitative importance of this molecule for brain development.

ACKNOWLEDGMENTS

We are grateful to Kyoung-Li Kim and Young-Ho Ahn for their expert technical assistance.

This work was supported in part by the Molecular Medicine Research Group Program (98-MM-01-01-A-02) and International Cooperative Research Program (1-04-006) from the Korean Ministry of Science and Technology and in part by grants from the Korea Science and Engineering Foundation, through the Protein Network Research Center. R.H.S. is a Hae-Eun LSRI investigator. H. Choi, C. Lee, and D. Shin were supported by the BK21 Research Fellowship from the Korea Ministry of Education.

REFERENCES

- Armstrong, J. A., and B. M. Emerson. 1998. Transcription of chromatin; these are complex times. *Curr. Opin. Genet. Dev.* **8**:165–172.
- Armstrong, J. F., M. H. Kaufman, D. J. Harrison, and A. R. Clarke. 1995. High-frequency developmental abnormalities in p53-deficient mice. *Curr. Biol.* **5**:931–936.
- Blackshear, P. J., W. S. Lai, J. S. Tuttle, D. J. Stumpo, E. Kennington, A. C. Nairn, and K. K. Sulik. 1996. Developmental expression of MARCKS and protein kinase C in mice in relation to the exencephaly resulting from MARCKS deficiency. *Dev. Brain Res.* **96**:62–75.
- Brizuela, B. J., L. Elfring, J. Billiard, J. W. Tamkun, and J. A. Kennison. 1994. Genetic analysis of the *brhma* gene of *Drosophila melanogaster* and polytene chromosome subdivisions 72AB. *Genetics* **137**:803–813.
- Brizuela, B. J., and J. A. Kennison. 1997. The *Drosophila* homeotic gene *moira* regulates expression of *engrailed* and *HOM* genes in imaginal tissues. *Mech. Dev.* **65**:209–220.
- Bultman, S., T. Gebuhr, D. Yee, C. L. Mantia, J. Nicholson, A. Gilliam, F. Randazzo, D. Metzger, P. Chambon, G. Crabtree, and T. Magnuson. 2000. A *Brg1* null mutation in the mouse reveals functional differences among mammalian SWI/SNF complexes. *Mol. Cell* **6**:1287–1295.
- Cairns, B. R., Y.-J. Kim, M. H. Sayre, B. C. Laurent, and R. D. Kornberg. 1994. A multisubunit complex containing the SWI1/ADR6, SWI2/SNF2, SWI3, SNF5, and SNF6 gene products isolated from yeast. *Proc. Natl. Acad. Sci. USA* **91**:1950–1954.
- Cairns, B. R., Y. Lorch, Y. Li, M. Zhang, L. Lacomis, H. Erdjument-Bromage, P. Tempst, J. Du, B. Laurent, and R. D. Kornberg. 1996. RSC, an essential, abundant chromatin-remodeling complex. *Cell* **87**:1249–1260.
- Chen, J., S. Chang, S. A. Duncan, H. J. Okano, G. Fishell, and A. Aderem. 1996. Disruption of the *MacMARCKS* gene prevents cranial neural tube closure and results in anencephaly. *Proc. Natl. Acad. Sci. USA* **93**:6275–6279.
- Cote, J., J. Quinn, J. L. Workman, and C. L. Peterson. 1994. Stimulation of GAL4 derivative binding to nucleosomal DNA by the yeast SWI/SNF complex. *Science* **265**:53–60.
- Crandall, J. E., M. Jacobson, and K. S. Kosik. 1986. Ontogenesis of microtubule-associated protein 2 (MAP2) in embryonic mouse cortex. *Brain Res.* **393**:127–133.
- Crosby, M. A., C. Miller, T. Alon, K. L. Watson, C. P. Verrijzer, R. Goldman-Lebi, and N. B. Zak. 1999. The *trithorax* group gene *moira* encodes a brahma-associated putative chromatin-remodeling factor in *Drosophila melanogaster*. *Mol. Cell. Biol.* **19**:1159–1170.
- Dingwall, A. K., S. J. Beek, C. M. McCallum, J. W. Tamkun, G. V. Kalpana, S. P. Goff, and M. P. Scott. 1995. The *Drosophila* *snr* and *brm* proteins are related to yeast SWI/SNF proteins and are components of a large protein complex. *Mol. Biol. Cell* **6**:777–791.
- Dunaief, J. L., B. E. Strober, S. Guha, P. A. Khavari, K. Alin, J. Luban, M. Begemann, G. R. Crabtree, and S. P. Goff. 1994. The retinoblastoma protein and BRG1 form a complex and cooperate to induce cell cycle arrest. *Cell* **79**:119–130.
- Elfring, L. K., R. Deuring, C. M. McCallum, C. L. Peterson, and J. W. Tamkun. 1994. Identification and characterization of *Drosophila* relatives of the yeast transcriptional activator SNF2/SWI2. *Mol. Cell. Biol.* **14**:2225–2234.
- Elfring, L. K., C. Daniel, O. Papoulas, R. Deuring, M. Sarte, S. Moseley, S. J. Beek, W. R. Waldrip, G. Daubresse, A. DePace, J. A. Kennison, and J. W. Tamkun. 1998. Genetic analysis of *brhma*: the *Drosophila* homolog of the yeast chromatin remodeling factor SWI2/SNF2. *Genetics* **148**:251–265.
- Guidi, C. J., A. T. Sands, B. P. Zambrowicz, T. K. Turner, D. A. Demers, W. Webster, T. W. Smith, A. N. Imbalzano, and S. N. Jones. 2001. Disruption of *Ini1* leads to peri-implantation lethality and tumorigenesis in mice. *Mol. Cell. Biol.* **21**:3598–3603.
- Harris, M. J., and D. M. Juriloff. 1999. Toward understanding mechanisms of genetic neural tube defects in mice. *Teratology* **60**:292–305.
- Hatini, V., W. Tao, and E. Lai. 1994. Expression of winged helix genes, *BF-1* and *BF-2*, define adjacent domains within the developing forebrain and retina. *J. Neurobiol.* **25**:1293–1309.
- Herrera, E., E. Samper, and M. A. Blasco. 1999. Telomere shortening in *mTR*^{-/-} embryos is associated with failure to close the neural tube. *EMBO J.* **18**:1172–1181.
- Hildebrand, J. D., and P. Soriano. 1999. Shroom, a PDZ domain-containing actin-binding protein, is required for neural tube morphogenesis in mice. *Cell* **99**:485–497.
- Hollander, M. C., M. S. Shaikh, D. V. Bulavin, K. Lundgren, L. Augeri-Hennmueller, R. Shehee, T. A. Molinaro, K. E. Kim, E. Tolosa, and J. D. Ashwell. 1999. Genomic instability in Gadd45a-deficient mice. *Nat. Genet.* **23**:176–184.
- Holstege, F. C. P., E. G. Jennings, J. J. Wyrick, T. I. Lee, C. J. Hengartner, M. R. Green, T. R. Golub, E. S. Lander, and R. A. Young. 1998. Dissecting the regulatory circuitry of a eukaryotic genome. *Cell* **95**:717–728.
- Huh, S., V. Hatini, R. C. Marcus, S. C. Li, and E. Lai. 1999. Dorsal-ventral patterning defects in the eye of *BF-1* deficient mice associated with a restricted loss of *shh* expression. *Dev. Biol.* **211**:53–63.
- Imbalzano, A. N. 1998. Energy-dependent chromatin remodelers: complex complexes and their components. *Crit. Rev. Eukaryot. Gene Expr.* **8**:225–255.
- Imhof, A., and A. P. Wolffe. 1998. Transcription: gene control by targeted histone acetylation. *Curr. Biol.* **8**:R422–R424.
- Jeon, S. H., M. G. Kang, Y. H. Kim, Y. H. Jin, C. Lee, H. Y. Chung, H. Kwon, S. D. Park, and R. H. Seong. 1997. A new mouse gene, *Srg3*, related to the *SWI3* of *Saccharomyces cerevisiae*, is required for apoptosis induced by glucocorticoids in a thymoma cell line. *J. Exp. Med.* **185**:1827–1836.
- Juriloff, D. M., and M. J. Harris. 2000. Mouse model for neural tube closure defects. *Hum. Mol. Genet.* **9**:993–1000.
- Kennison, J. A., and J. W. Tamkun. 1988. Dosage-dependent modifiers of *Polycomb* and *Antennapedia* mutations in *Drosophila*. *Proc. Natl. Acad. Sci. USA* **85**:8136–8140.
- Kingston, R. E., and G. J. Narlikar. 1999. ATP-dependent remodeling and acetylation as regulators of chromatin fluidity. *Genes Dev.* **13**:2339–2352.
- Klochendler-Yeivin, A., L. Fiette, J. Barra, C. Muchardt, C. Babinet, and M. Yaniv. 2000. The murine SNF5/INI1 chromatin remodeling factor is essential for embryonic development and tumor suppression. *EMBO Rep* **1**:500–506.
- Koleske, A. J., A. M. Gifford, M. L. Scott, M. Nee, and R. T. Bronson. 1998.

- Essential roles for the Abl and Arg tyrosine kinases in neurulation. *Neuron* **21**:1259–1272.
33. Kornberg, R. D., and Y. Lorch. 1999. Twenty-five years of the nucleosome, fundamental particle of the eukaryote chromosome. *Cell* **98**:285–294.
 34. Lanier, L. M., M. A. Gates, W. Witke, A. S. Menzies, and A. M. Wehman. 1999. Mena is required for neurulation and commissure formation. *Neuron* **22**:313–325.
 35. Legouy, E., E. M. Thompson, C. Muchardt, and J. P. Renald. 1998. Differential preimplantation regulation of two mouse homologs of the yeast SWI2 protein. *Dev. Dyn.* **212**:38–48.
 36. Muchardt, C., and M. Yaniv. 1999. The mammalian SWI/SNF complex and the control of cell growth. *Semin. Cell Dev. Biol.* **10**:189–195.
 37. Papoulas, O., S. J. Beek, S. L. Moseley, C. M. McCallum, M. Sarte, A. Shearn, and J. K. Tamkun. 1998. The *Drosophila* trithorax group proteins BRM, ASH, and ASH are subunits of distinct protein complexes. *Development* **125**:3955–3966.
 38. Peterson, C. L., and I. Herskowitz. 1992. Characterization of the yeast *SWI1*, *SWI2*, *SWI3* genes, which encode a global activator of transcription. *Cell* **68**:573–583.
 39. Peterson, C. L., A. Dingwall, and M. P. Scott. 1994. Five SWI/SNF gene products are components of a large multisubunit complex required for transcriptional enhancement. *Proc. Natl. Acad. Sci. USA* **91**:2905–2908.
 40. Peterson, C. L. 1996. Multiple SWI/SNFs to turn on chromatin? *Curr. Opin. Genet. Dev.* **6**:171–175.
 41. Phelan, M. L., S. Sif, G. J. Narlikar, and R. E. Kingston. 1999. Reconstitution of a core chromatin remodeling complex from SWI/SNF subunit. *Mol. Cell.* **3**:247–253.
 42. Randazzo, F. M., M. Khavari, G. Crabtree, J. Tamkun, and J. Rossant. 1994. *brg1*: a putative murine homologue of the *Drosophila brahma* gene, a homeotic gene regulator. *Dev. Biol.* **161**:229–242.
 43. Reyes, J. C., J. Barra, C. Muchardt, A. Camus, C. Babinet, and M. Yaniv. 1998. Altered control of cellular proliferation in the absence of mammalian brahma (SNF2 α). *EMBO J.* **17**:6979–6991.
 44. Roberts, C. W., S. A. Galusha, M. E. McMenamin, C. D. Fletcher, and S. H. Orkin. 2000. Haploinsufficiency of Snf5 (integrator interactor 1) predisposes to malignant rhabdoid tumors in mice. *Proc. Natl. Acad. Sci. USA* **97**:13796–13800.
 45. Sadler, T. W., D. Greenberg, P. Coughlin, and J. L. Lessard. 1982. Actin distribution patterns in the mouse neural tube during neurulation. *Science* **215**:172–174.
 46. Sah, V. P., L. D. Attardi, G. J. Mulligan, B. O. Williams, R. T. Bronson, and T. Jacks. 1995. A subset of p53-deficient embryos exhibit exencephaly. *Nat. Genet.* **10**:175–180.
 47. Shanahan, F., W. Seghezzi, D. Parry, D. Mahony, and E. Lees. 1999. Cyclin E associates with BAF155 and BRG1, components of the mammalian SWI-SNF complex, and alters the ability of BRG1 to induce growth arrest. *Mol. Cell. Biol.* **19**:1460–1469.
 48. Sif, S., P. T. Stukenberg, M. W. Kirschner, and R. E. Kingston. 1998. Mitotic inactivation of a human SWI/SNF chromatin remodeling complex. *Genes Dev.* **12**:2842–2851.
 49. Soriano, P. 1997. The PDGF receptor is required for neural crest cell development and for normal patterning of the somites. *Development* **124**:2691–2700.
 50. Strober, B. E., J. L. Dunaief, S. Guha, and S. P. Goff. 1996. Functional interactions between the hBRM/hBRG1 transcriptional activators and the pRB family of proteins. *Mol. Cell. Biol.* **16**:1576–1583.
 51. Struhl, K. 1999. Fundamentally different logic of gene regulation in eukaryotes and prokaryotes. *Cell* **98**:1–4.
 52. Stumpo, D. J., C. B. Bock, J. S. Tuttle, and P. J. Blackshear. 1995. MARCKS deficiency in mice leads to abnormal brain development and perinatal death. *Proc. Natl. Acad. Sci. USA* **92**:944–948.
 53. Sudarsanam, P., and F. Winston. 2000. The Swi/Snf family nucleosome-remodeling complexes and transcriptional control. *Trends Genet.* **16**:345–351.
 54. Tamkun, J. W., R. Deuring, M. P. Scott, M. Kissinger, A. M. Pattatucci, T. C. Kaufman, and J. A. Kennison. 1992. Brahma: a regulator of *Drosophila* homeotic genes and structurally related to the yeast transcriptional activator SNF2/SWI2. *Cell* **68**:561–572.
 55. Tamkun, J. W. 1995. The role of brahma and related proteins in transcription and development. *Curr. Opin. Genet. Dev.* **5**:473–477.
 56. Varga-Weisz, P. D., and P. B. Becker. 1998. Chromatin-remodeling factors: machines that regulate? *Curr. Opin. Cell Biol.* **10**:346–353.
 57. Vignali, M., A. H. Hassan, K. E. Neely, and J. L. Workman. 2000. ATP-dependent chromatin-remodeling complexes. *Mol. Cell. Biol.* **20**:1899–1910.
 58. Wang, W., J. Cote, Y. Xue, S. Zhou, P. A. Khavari, S. R. Biggar, C. Muchardt, G. V. Kalpana, S. P. Goff, M. Yaniv, J. L. Workman, and G. R. Crabtree. 1996. Purification and biochemical heterogeneity of the mammalian SWI-SNF complex. *EMBO J.* **15**:5370–5382.
 59. Wang, W., Y. Xue, S. Zhou, A. Kuo, B. R. Cairns, and G. R. Crabtree. 1996. Diversity and specialization of mammalian SWI/SNF complex. *Genes Dev.* **10**:2117–2130.
 60. Winston, F., and M. Carlson. 1992. Yeast SNF/SWI transcriptional activators and the SPT/SIN chromatin connection. *Trends Genet.* **8**:387–391.
 61. Wu, M., D. F. Chen, T. Sasaoka, and S. Tonegawa. 1996. Neural tube defects and abnormal brain development in F52-deficient mice. *Proc. Natl. Acad. Sci. USA* **93**:2110–2115.
 62. Xu, W., H. Baribault, and E. D. Adamson. 1998. Vinculin knockout results in heart and brain defects during embryonic development. *Development* **125**:327–337.
 63. Xuan, S., C. Baptista, G. Balas, W. Tao, V. Soares, and E. Lai. 1995. Winged helix transcription factor BF-1 is essential for the development of the cerebral hemispheres. *Neuron* **14**:1141–1152.
 64. Zhang, S. H., M. Gavin, A. Dahiya, A. A. Postigo, D. Ma, R. X. Luo, J. W. Harbour, and D. C. Dean. 2000. Exit from G1 and S phase of the cell cycle is regulated by repressor complexes containing HDAC-Rb-hSWI/SNF and Rb-hSWI/SNF. *Cell* **101**:79–89.